

# GaN Heterostructure Barrier Diodes Exploiting Polarization-Induced $\delta$ -Doping

Pei Zhao, Amit Verma, Jai Verma, Huili Grace Xing, Patrick Fay, and Debdeep Jena

**Abstract**—A GaN-based heterostructure barrier diode (HBD) similar to GaAs planar-doped barrier diodes is demonstrated. Instead of doping with impurities, the polarization-induced sheet charge at the III-nitride heterojunction behaves as an effective  $\delta$ -doping. An AlGaIn/GaN heterostructure is used for the demonstration. The rectifying characteristics of the polarization-induced GaN HBDs can be tuned by controlling the graded AlGaIn thickness and composition. Such polarization-engineered HBDs can find applications in high-voltage and high-frequency electronics.

**Index Terms**—Aluminum nitride, gallium nitride, polarization doping, heterostructure, planar doped barrier, MBE.

## I. INTRODUCTION

THE nonlinear characteristics of solid-state devices such as mixers, detectors, and frequency multipliers are widely used for high frequency applications [1]–[3]. Improved flexibility in device design while retaining a rectifying I-V can be realized by p-type  $\delta$ -doping in the middle of an intrinsic GaAs layer sandwiched between n-type cathode and anode. The device is known as the Planar Doped Barrier (PDB) diode [4]. The barrier height and the depletion region thickness are decided by the position and concentration of the  $\delta$ -doping. The performance of the PDB diode is limited by the control of  $\delta$ -doping. In III-Nitride heterostructures, due to the presence of a high spontaneous and piezoelectric polarization charge, an effective  $\delta$ -doping can be induced at sharp heterojunctions with atomic control and doping densities far beyond what is achievable by chemical acceptor (or donor)  $\delta$ -doping [5]. This letter presents the demonstration of PDB technology in a III-Nitride heterostructure by exploiting polarization-induced sheet charge.

## II. EXPERIMENTS

The GaN HBD layer structure is shown in Fig. 1(a). The heterostructure consists of a heavily doped  $n^+$  GaN contact layer at the bottom, followed by a linearly graded AlGaIn layer, followed by an UID GaN layer and an  $n^+$  GaN contact layer on top. The net charge distribution and energy band diagram

Manuscript received March 11, 2014; accepted March 31, 2014. Date of publication April 18, 2014; date of current version May 20, 2014. This work was supported by the Office of Naval Research through the DATE MURI Program (Dr. Paul Maki). The review of this letter was arranged by Editor T. Egawa.

The authors are with the Department of Electrical Engineering, University of Notre Dame, Notre Dame, IN 46556 USA (e-mail: djena@nd.edu).

Color versions of one or more of the figures in this letter are available online at <http://ieeexplore.ieee.org>.

Digital Object Identifier 10.1109/LED.2014.2316140

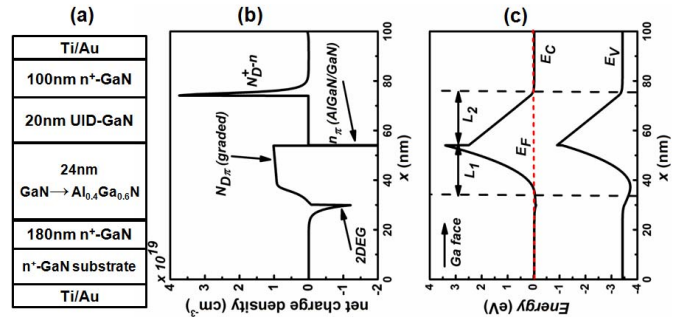


Fig. 1. (a) structure of GaN heterostructure barrier diode with contact metals. (b) net charge density distribution with bulk polarization charge in the graded region and, polarization sheet charge at AlGaIn/GaN interface. (c) Energy band diagram of the active region and the contact layers at zero bias.

are calculated self-consistently by solving Schrodinger and Poisson equations [6] [Fig. 1(b), (c)]. The compositionally graded AlGaIn has a non-vanishing divergence of polarization. The linear grading results in an approximately constant polarization charge as  $\rho = -\nabla \cdot \vec{P}$ , where  $\vec{P}$  is the total polarization,  $\rho = qN_{D\pi}$  and  $N_{D\pi}$  is the positive bulk fixed polarization charge in the graded AlGaIn region [Fig. 1(b)]. To satisfy the global charge neutrality, a sheet charge exists at the abrupt AlGaIn/UID GaN heterojunction [7]

$$\sigma_{\pi} = qN_{D\pi}t = qn_{\pi}, \quad (1)$$

where  $\sigma_{\pi}$  is the polarization sheet charge at the Al<sub>x</sub>Ga<sub>1-x</sub>N/GaN interface,  $q$  is the electron charge and  $t$  is the thickness of the graded Al<sub>x</sub>Ga<sub>1-x</sub>N. With  $x = 0.4$  and  $t = 24$ nm, the corresponding  $N_{D\pi} \sim 9.4 \times 10^{18}$ cm<sup>-3</sup>. A fixed negative polarization sheet charge  $n_{\pi} \sim 2.26 \times 10^{13}$ cm<sup>-2</sup> is located at the interface of Al<sub>0.4</sub>Ga<sub>0.6</sub>N/GaN junction. The existence of the sheet charge induces a potential barrier for electrons as shown in Fig. 1(c). By increasing the Al composition, polarization induced sheet charge density can be as high as  $6.1 \times 10^{13}$ cm<sup>-2</sup>, but *without* real acceptor doping.

The corresponding heterostructure is grown by plasma-assisted molecular beam epitaxy (MBE) in a Veeco Gen 930 system. A Ga-face  $n^+$  bulk GaN substrate from Ammono with dislocation density  $<10^5$ cm<sup>-2</sup> [8] is used. Two epitaxial structures with different Al composition in graded GaN  $\rightarrow$  Al<sub>x</sub>Ga<sub>1-x</sub>N ( $x = 0.4$  and  $x = 0.75$ ) were grown. The material characterization is presented for HBDs with  $x = 0.4$ . The cross-section scanning transmission electron microscopy (STEM) image of the completed GaN HBD is shown in Fig. 2. A 180 nm  $n^+$ GaN has

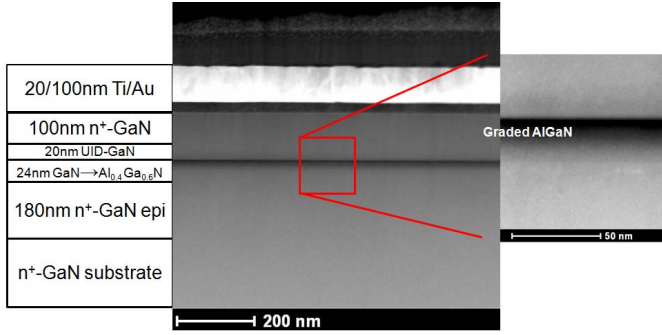


Fig. 2. Sketch of GaN heterostructure barrier diode with the corresponding STEM picture. The growth interface between bulk substrate and epitaxial layer is invisible. The atomic fraction of Al is linearly changing in the graded region.

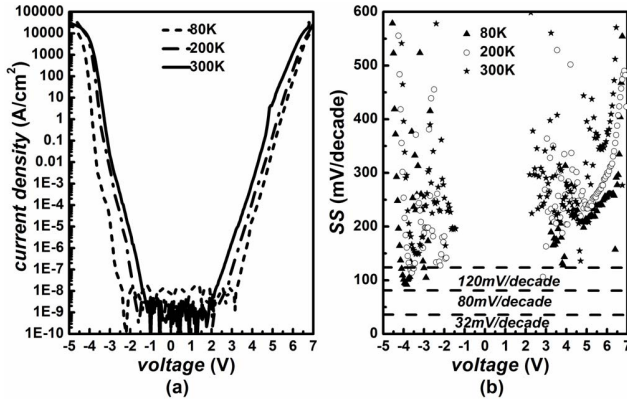


Fig. 3. (a) IV characteristics at 300K, 200K and 80K of HBD with graded  $\text{Al}_{0.4}\text{Ga}_{0.6}\text{N}$  in semi-log scale (b) SS vs. the voltage of the same device.

been grown first followed by the graded AlGaIn region. The atomic fraction of Al in the graded region is linear as confirmed by secondary ion mass spectrometry (SIMS) and energy-dispersive X-ray spectroscopy (EDX) analysis. The Si doping in the anode and cathode  $n^+\text{GaN}$  is  $\sim 3 \times 10^{19}\text{cm}^{-3}$ , and the background concentration in the 20nm UID-GaN is  $\sim 1 \times 10^{17}\text{cm}^{-3}$ . The STEM figure confirms the successful realization of the heterostructure required for GaN HBDs with the compositionally graded AlGaIn layer without visible extended defects or dislocations inside measured diodes. The anode of the diode is a circle of  $10\mu\text{m}$  radius defined by reactive-ion etching (RIE) mesa isolation. The cathode is a back contact on the  $n^+\text{GaN}$  bulk substrate.

### III. RESULTS AND DISCUSSION

The expected I-V characteristics of the GaN HBD closely follows the thermionic emission model developed for GaAs PDB diodes [9]

$$I = A^*T^2 \exp\left(-\frac{q\phi_B}{k_B T}\right) \left[ \exp\left(\frac{q\alpha_1 V}{k_B T}\right) - \exp\left(\frac{q\alpha_2 V}{k_B T}\right) \right], \quad (2)$$

where  $A^*$  is the Richardson constant,  $T$  is the temperature,  $\Phi_B$  is the zero-bias barrier height,  $k_B$  is the Boltzmann constant,  $L_1(L_2)$  is the depletion region thickness on the left (right) side of the barrier as shown in Fig. 1(c), and the ‘lever’ rule ratios are  $\alpha_1 = L_1/(L_1 + L_2)$ ,  $\alpha_2 = L_2/(L_1 + L_2)$ .

The measured I-V characteristic of a GaN HBD with a 24nm  $\text{GaN} \rightarrow \text{Al}_{0.4}\text{Ga}_{0.6}\text{N}$  graded region ( $L_1$ ) and 20nm

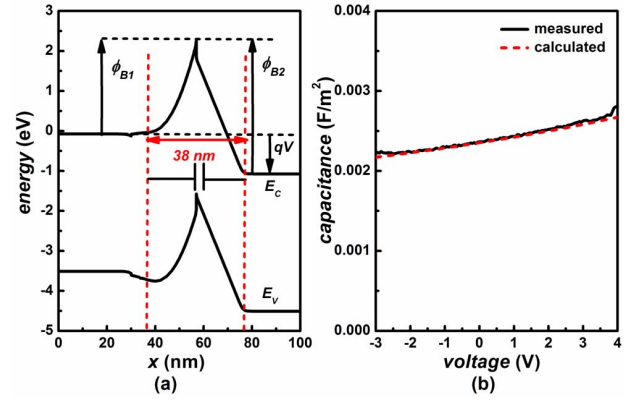


Fig. 4. Band diagrams of GaN HBD with 24nm graded  $\text{Al}_{0.4}\text{Ga}_{0.6}\text{N}$  (20nm UID-GaN) at 1V. (b) CV of the same device.

UID-GaN ( $L_2$ ) is shown in Fig. 3(a). The modulation is more than 13 orders of magnitude. The bulk substrates and homoepitaxy eliminate dislocation related leakage, allowing a thorough exploration of the HBD physics. The near-symmetric I-V characteristics are due to the similar depletion region thicknesses  $L_1 = L_2$ , with  $\alpha_1 = \alpha_2 = 0.5$ . The expected subthreshold swing (SS) is close to the expected values at 300K, 200K and 80K (dashed lines highlight the expected value) as shown in Fig. 3(b). The built-in electric field in the depleted region is  $\sim 1.1\text{MV/cm}$  at zero bias, which increases to  $2\sim 4\text{MV/cm}$  at high biases. The contribution of field-assisted tunneling at high biases increases the current and changes the expected thermionic SS. The rigorous analysis of the transport process will be presented later.

Fig. 4(a) shows the energy band diagram of the same device as Fig. 3, at the bias of 1 V. Fig. 4(b) shows the measured capacitance (solid line) compared with expected capacitance of the depleted region (dashed line). Similar to GaAs PDB diodes, the depletion region thickness does not vary appreciable with bias, and the measured capacitance at zero bias is the parallel-plate capacitance of the depleted AlGaIn/GaN heterostructure. The bias dependent CV calculated by solving the charge neutrality equation and continuity of conduction band edge. It matches well with the measured data [dashed line in Fig. 4(b)].

The electron barrier in these HBDs is induced by the polarization charge. The barrier height can be estimated to be

$$\phi_B = \frac{N_{D\pi} L_1^2}{2\epsilon_S \epsilon_0}, \quad (3)$$

where  $L_1$  is the depletion thickness of the graded AlGaIn,  $N_{D\pi}$  is the bulk fixed polarization charge in the graded AlGaIn region,  $\epsilon_0$  is the vacuum permittivity, and  $\epsilon_S$  is the dielectric constant of AlGaIn. Fig. 5(a) shows the change of barrier height at different Al compositions with a fixed graded AlGaIn thickness  $t = 24\text{nm}$ . The bias-dependent barrier height is

$$\phi_{B1}(V) = \phi_B - \frac{L_1}{L_1 + L_2} V, \quad (4)$$

$$\phi_{B2}(V) = \phi_B + \frac{L_2}{L_1 + L_2} V, \quad (5)$$

where  $V$  is the external bias,  $\Phi_{B1}$  and  $\Phi_{B2}$  are the barriers for right going and left going electrons as sketched in Fig. 4(a).

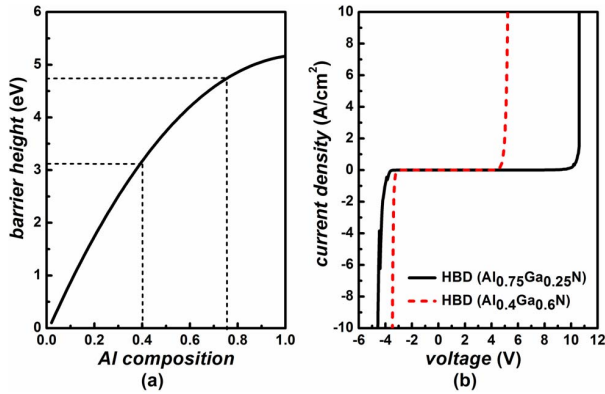


Fig. 5. (a) Estimated barrier height at different Al composition with a fixed graded region thickness of 24nm. (b) Comparison of the IV characteristics of the HBD with Al composition at 40% and 75% in the graded region.

The forward bias turn on voltage is the bias required for reaching a flat band at  $\Phi_{B1}$ , which is about 6V and 9.5V corresponding to 40% and 75% Al composition in graded AlGaIn. The IV characteristics of a 75% graded HBD is compared with the 40% HBD in Fig. 5(b). The turn-on voltages are close to the predicted values, proving the feasibility of polarization-based design of such devices.

GaN HBDs could be used for high frequency applications as mixers and detectors, as has already been demonstrated for GaAs PDB diodes [10], [11]. A figure-of-merit for detector applications is the curvature coefficient

$$\gamma = \frac{\partial^2 I / \partial V^2}{\partial I / \partial V}. \quad (6)$$

Based on equation (2), the ideal curvature coefficient of a GaN HBD is  $q\alpha_i/k_B T$ , where  $i = 1, 2$  depends on the diode either in the forward bias or backward bias. At 300K, the peak curvature coefficient based on the I-V in Fig. 3(a) is  $16 \text{ V}^{-1}$ , which is close to the expected value of  $19 \text{ V}^{-1}$ . An asymmetric HBD ( $L_2 \gg L_1$ ) will behave as a backward diode with  $\alpha \sim 1$  and the curvature coefficient will be close to the ideal curvature coefficient  $q/k_B T \sim 38 \text{ V}^{-1}$  of a Schottky barrier.

One advantage of GaN HBD could be the constant capacitance, which reduces the nonlinearity of the device. In GaN HBDs, the series resistance and junction capacitance can

be independently minimized through control of barrier height and width. Thus the RC constant smaller than a Schottky diode may be feasible. As a majority carrier device, GaN HBD could offer high switching speeds than p-i-n diodes due to the absence of minority carriers.

#### IV. CONCLUSION

In conclusion, this letter demonstrates GaN based heterostructure barrier diodes with polarization-induced  $\delta$ -doping at graded AlGaIn/GaN heterointerfaces. Tunable rectifying IV characteristics is achieved by accurate composition and thickness control in epitaxy, and letting the built-in polarization charges at sharp heterojunctions take over the role of chemical dopants.

#### REFERENCES

- [1] S. A. Maas, *Microwave Mixers*. Norwood, MA, USA: Artech House, 1986.
- [2] N. Su *et al.*, "Sb-heterostructure millimeter-wave detectors with reduced capacitance and noise equivalent power," *IEEE Electron Device Lett.*, vol. 29, no. 6, pp. 536–539, Jun. 2008.
- [3] Z. Zhang *et al.*, "Sub-micron area heterojunction backward diode millimeter-wave detectors with  $0.18 \text{ pW/Hz}^{1/2}$  noise equivalent power," *IEEE Microw. Wireless Compon. Lett.*, vol. 21, no. 5, pp. 267–269, May 2011.
- [4] R. J. Malik *et al.*, "Planar-doped barriers in GaAs by molecular beam epitaxy," *Electron. Lett.*, vol. 16, no. 22, pp. 836–838, 1980.
- [5] P. Zhao *et al.*, "GaN heterostructure barrier diodes (HBD) with polarization-induced delta-doping," in *Proc. IEEE Device Res. Conf.*, Jun. 2013.
- [6] (2013). *The Software Is Available from the Webpage of Prof. Gregory Snider at University of Notre Dame* [Online]. Available: <http://www.nd.edu/gsniderS>
- [7] C. Wood and D. Jena, *Polarization Effects in Semiconductors: From Ab Initio Theory to Device Applications*. New York, NY, USA: Springer-Verlag, 2008.
- [8] AMMONO [Online]. Available: <http://www.ammono.com/products>, Version: 20110906
- [9] S. M. Sze, *High-Speed Semiconductor Devices*. New York, NY, USA: Wiley, 1990.
- [10] M. J. Kearney, A. Condie, and I. Dale, "GaAs planar doped barrier diodes for millimetre-wave detector applications," *Electron. Lett.*, vol. 27, no. 9, pp. 721–722, 1991.
- [11] R. J. Malik and S. Dixon, "A subharmonic mixer using a planar doped barrier diode with symmetric conductance," *IEEE Electron Device Lett.*, vol. 3, no. 7, pp. 205–207, Jul. 1982.